

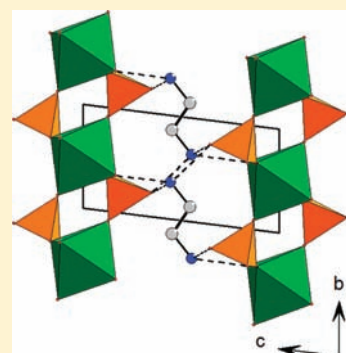
Linear Alkyl Diamine-Uranium-Phosphate Systems: U(VI) to U(IV) Reduction with Ethylenediamine

Laurent Jouffret, Murielle Rivenet,* and Francis Abraham

Unité de Catalyse et de Chimie du Solide, UCCS-UMR 8181, ENSCL/USTL, Bât. C7, BP 90108, 59652 Villeneuve d'Ascq cedex, France

S Supporting Information

ABSTRACT: Mild-hydrothermal reactions in acidic medium using 1,3-diaminopropane, 1,4-diaminobutane, and 1,5-diaminopentane as structure directing agents led to three-dimensional (3D) uranyl phosphates $(\text{CH}_2)_3(\text{NH}_3)_2\{[(\text{UO}_2)(\text{H}_2\text{O})][(\text{UO}_2)(\text{PO}_4)]_4\}$ (C3USP4), $(\text{CH}_2)_4(\text{NH}_3)_2\{[(\text{UO}_2)(\text{H}_2\text{O})][(\text{UO}_2)(\text{PO}_4)]_4\}$ (C4USP4) and $(\text{CH}_2)_5(\text{NH}_3)_2\{[(\text{UO}_2)(\text{H}_2\text{O})][(\text{UO}_2)(\text{PO}_4)]_4\}$ (C5USP4). The structures of (C4USP4) and (C5USP4) were solved in the space group $Cmc2_1$ using single-crystal X-ray diffraction data. The compounds are isostructural to the corresponding uranyl vanadates and contain the same 3D inorganic framework built from uranyl-phosphate layers of uranophane-type anion topology pillared by $[\text{UO}_6(\text{H}_2\text{O})]$ pentagonal bipyramids. In neutral or basic medium the alkyl diamines decompose to give ammonium uranyl phosphate trihydrate. In the same conditions by using ethylenediamine, unexpected reduction of uranium(VI) to uranium(IV) occurs leading to the formation of $(\text{CH}_2)_2(\text{NH}_3)_2[\text{U}(\text{PO}_4)_2]$ (C2UP2) single crystals. C2UP2 undergoes a reversible phase transition from triclinic to monoclinic symmetry at about 230 °C. The structure of the two forms results from the stacking of inorganic layers $\infty^1[\text{U}(\text{PO}_4)_2]^{2-}$, and organic layers containing ethylene diammonium ions, the two layers being linked by hydrogen bonds. Single crystals of $(\text{CH}_2)_2(\text{NH}_3)_2[\text{PO}_3\text{OH}]$ (C2HP) are formed by evaporation of the solution after filtering of C2UP2 single crystals. The structure of C2HP contains infinite $\infty^1[\text{PO}_3\text{OH}]^{2-}$ chains connected by $(\text{CH}_2)_2(\text{NH}_3)_2^{2+}$ ions through hydrogen bonds.



INTRODUCTION

Uranium compounds have been the subject of an increased attention this past decade because of their importance in the nuclear fuel cycle and nuclear waste management and because of their exciting chemistry. In inorganic compounds uranium presents the two main oxidation states U(IV) and U(VI); however, it is mainly contained as U(VI), which often occurs as an approximately linear uranyl dioxo cation in natural and synthetic compounds.¹ The large number of published papers focusing on the solid state chemistry of uranyl-containing inorganic compounds illuminates the originality of the crystal chemistry of this ion and the diversity of structural arrangements when it is associated with oxoanions such as silicate, phosphate, vanadate, molybdate, tungstate. The basic building units are the uranium polyhedra, which can be square-, pentagonal-, or hexagonal bipyramids, formed by uranyl ions surrounded in the equatorial planes by 4, 5, or 6 oxygen atoms,¹ and the oxoanion which can be essentially a tetrahedron, square pyramid, or octahedron. The structural arrangement depends on many factors, such as the U/oxoanion ratio, which influences the degree of polymerization between the uranium polyhedra either connected directly through equatorial oxygen atoms or through the oxoanion polyhedra. There is a strong tendency to form layered structures because of the presence of uranyl bonds that are aligned in a parallel fashion and preclude the connection in a third dimension. For example, the natural minerals with $\text{UO}_2/\text{XO}_n = 1$ ($X = \text{P}, \text{As}, \text{V}, \text{Si}$) are all

bidimensional compounds exhibiting different types of layers according to the uranium-oxoanion (XO_n) systems. The autunite layer, obtained for $X = \text{P}$ and As , is built from UO_6 octahedra and XO_4 tetrahedra. The carnotite layer ($X = \text{V}$) is built from UO_7 pentagonal bipyramids and VO_5 square pyramid while the uranophane layer ($X = \text{Si}$) is built from UO_7 pentagonal bipyramids and SiO_4 tetrahedra. The stable layers which occur naturally in the considered system such as autunite and carnotite layers for $X = \text{As}$ and V , can be synthesized in the presence of amine like 1,4-diazabicyclo[2,2,2]octane (*Dabco*, $\text{N}_2\text{C}_6\text{H}_{12}$),^{2,3} but the use of other organic structure directing agents such as triethylamine ($\text{N}(\text{C}_2\text{H}_5)_3$) and piperazine ($\text{N}_2\text{C}_4\text{H}_{10}$) can form the unexpected uranophane-type layers both for $X = \text{As}^2$ and V^3 . Furthermore three-dimensional (3D) frameworks with $\text{U}/\text{X} = 3/2, 5/4$, and $4/3$ were obtained by linking the uranophane-type layers through various numbers of UO_7 or UO_6 uranyl pillars. The neutral framework $\{(\text{UO}_2)[(\text{UO}_2)(\text{XO}_4)]_2\}$ ($\text{U}/\text{X} = 3/2$) was obtained for $X = \text{V},^4 \text{P},^5 \text{As}^6$. In these compounds, the structural arrangement creates perpendicular channels occupied by water molecules. The ratio $\text{U}/\text{X} = 5/4$, which corresponds to an anionic framework of formula $\{(\text{UO}_2)[(\text{UO}_2)(\text{XO}_4)]_4\}^{2-}$, was obtained using either alkali metals: K ($X = \text{P}$),⁷ Rb and Cs ($X = \text{P}, \text{As}$),⁸ Tl ($X = \text{P}$)⁹ or amines such as piperazine or

Received: February 18, 2011

Published: April 15, 2011

diethylamine ($X = P$),^{2,10} dimethylamine, pyridine, or linear alkyl diamines ($n = 3-7$) ($X = V$).^{11,12} The ratio $U/X = 4/3$, $\{(UO_2)[(UO_2)(XO_4)]_3\}^-$, was generated by using isopropylamine, tetramethylamine, cyclohexylamine, and tertbutylamine and reported only for $X = V$.¹¹ So, for $X = V$, a series formulated $A_{2x/n}\{(UO_2)_{1-x}[(UO_2)(XO_4)]_2\}$ was finally proposed with x being equal to 0, 1/3, 1/2, or 1 (layered compounds) and $n = 1$ (monoprotonated amine or alkali metal) or 2 (diprotonated amines).¹³ The composition and the crystal structure of these compounds depend on the uranophane-type layer geometric isomer provided by the orientation of the successive XO_4 tetrahedra. The various geometric isomers of the uranophane-type layer were introduced by Locock and Burns⁶ and recently completed.¹³ They can be related to the nature and size of the monovalent or divalent cation A and to the nature of X . For example, $A_2[UO_2(H_2O)[(UO_2)(PO_4)]_4] \cdot H_2O$, obtained for $x = 1/2$ and $X = P$, exhibits two different structures corresponding to the two geometric isomers of the uranophane-type layer (uudd/dduu) for $A = K, Rb, Tl$ ^{7,9} and (uudd/uddu) for $A = Cs$.⁷ This last geometric isomer can also be found in the uranyl-vanadates $(CH_2)_n(NH_3)_2[UO_2(H_2O)[(UO_2)(VO_4)]_4] \cdot mH_2O$ where $(CH_2)_n(NH_3)_2^{2+}$ are diprotonated linear alkyl diamines ($n = 3-7$).¹² This paper reports the study of the uranium-phosphate-linear alkyl diamine systems according to the hydrothermal synthesis conditions (acidic, neutral and basic) and the unexpected reduction of U(VI) to U(IV) in presence of ethylenediamine.

EXPERIMENTAL SECTION

Synthesis. Three series of experiments were realized, in acidic, neutral and basic medium, respectively, in the same hydrothermal conditions. For the first series, the reactants were solid uranyl nitrate $(UO_2(NO_3)_2 \cdot 6H_2O)$ Prolabo, R.P. normapur, 100.4 mg, 0.2 mmol), phosphoric acid as a source of phosphate ions (H_3PO_4 , Carlo Erba, 5 mL of a 1 mol/L solution, 5 mmol), nitric acid (HNO_3 , Merck, 5 mL of a 1 mol/L solution, 5 mmol) and a solution of the considered linear alkyl diamine $(NH_2)(CH_2)_n(NH_2)$ with $2 \leq n \leq 7$ (2.5 mL of a 0.2 mol/L solution, 0.5 mmol) obtained by dissolution of the commercial products in deionized water, 1,2-diaminoethane (Alfa Aesar 99%, $d = 0.899$), 1,3-diaminopropane (Acros 99%, $d = 0.888$), 1,4-diaminobutane (Aldrich 99%, $d = 0.877$), 1,5-diaminopentane (Acros 98%, $d = 0.87$), 1,6-diaminohexane (Acros 99.5%), 1,7-diaminoheptane (Acros 98%) leading to $pH \approx 0.3$. For the second and third series, highly concentrated solutions of diamine (14.5, 11.8, 11.65, 8.55, 8.835, 7.865 mol/L for $n = 2$ to 7, respectively) were used directly. The volume of added diamine was adjusted so as to obtain a pH value of about 7 ($V \sim 0.6$ mL) and 11 ($V \sim 2$ mL), respectively for the neutral and basic conditions. The reactants were introduced into 23 mL Teflon-lined Parr steel autoclaves and heated at 190 °C in a Thermo Scientific Heraeus oven for 6 days and then slowly cooled (1 °C/h) to room temperature. The precipitated solids were collected by filtration and washed using deionized water before analysis.

In acidic medium, no precipitate was obtained by using 1,2-diaminoethane, only a green solution results from the hydrothermal treatment. By using 1,3-diaminopropane, 1,4-diaminobutane, and 1,5-diaminopentane, single crystals of $(CH_2)_n(NH_3)_2\{UO_2(H_2O)[(UO_2)(PO_4)]_4\} \cdot mH_2O$ (denoted hereafter $CnUSP4$, with $n = 3, 4, 5$ respectively) were obtained. They are accompanied with single crystals of $(UO_2)[(UO_2)(PO_4)]_2 \cdot 4H_2O$ ⁵ and powder of $\alpha-U_3O_8$ precluding determination of reaction yields. By using 1,6-diaminohexane and 1,7-diaminoheptane powder of ammonium uranyl phosphate trihydrate, $(NH_4)[(UO_2)(PO_4)] \cdot 3H_2O$ (PDF no. 42-0384)¹⁴ is obtained. In neutral medium, powder of ammonium uranyl phosphate trihydrate is formed when using the alkyl

diamines with $n = 3$ to 7 whereas hydrogen uranyl phosphate tetrahydrate¹⁵ (PDF no. 37-0367) is obtained for diamine with $n = 2$ (1,2-diaminoethane or ethylenediamine). In basic medium, ammonium uranyl phosphate trihydrate accompanied by an unidentified poorly crystallized phase is synthesized by means of using $(CH_2)_n(NH_3)_2$ diamines containing 3 to 7 carbons in the alkyl linear chain. On the contrary, with ethylenediamine, pink single crystals of a new compound $(CH_2)_2(NH_3)_2-[U(PO_4)_2]$ (C2UP2) were obtained (yield = 45%). The evaporation of the resulting solution allowed the crystal growth of the ethylenediamine hydrogenophosphate $(CH_2)_2(NH_3)_2(PO_3OH)$ (C2HP) compound.

Crystal Structure Determination. Single crystals were isolated under an optical microscope. The selected crystals were mounted on a glass fiber and aligned on a 3 circles Bruker SMART diffractometer equipped with a CCD detector (SMART-1K-CCD or BRUKER AXS APEX2 CCD-4K) for single-crystal X-ray diffraction experiments. Intensities were collected using MoK α radiation selected by a graphite monochromator. Between 2718 and 4240 frames were collected to cover the full sphere. The individual frames of the single crystals of $CnUSP4$ ($n = 3-5$) were measured at 100 K using an OXFORD Cryosystem CRYOSTREAM and an Ω -scan technique while those of the single crystals of C2UP2 and C2HP were measured at room temperature using an optimized Φ and Ω -scan collection strategy (COSMO BRUKER program¹⁶). Acquisition time was fixed in the range 20 to 60 s/frame according to the crystal dimensions and intensities.

The BRUKER program SAINT¹⁷ was used for intensity data integration and correction for Lorentz, polarization, and background effects. After data processing, absorption corrections were performed using a semiempirical method based on redundancy with the SADABS program.¹⁸ The crystal structures were solved in the non-centrosymmetric space group $Cmc2_1$ for $CnUSP4$ ($n = 4, 5$) and in centrosymmetric space groups $P\bar{1}$ and $P2_1/c$ for C2UP2 and C2HP, respectively. The structures for $CnUSP4$ ($n = 4, 5$) were twinned by inversion. The twin fractions are given in Table 1. The poor quality of the C3USP4 single crystals did not allow a complete and satisfactory crystal structure determination, only the inorganic framework can be asserted, so its crystal structure determination is not reported in this paper.

The single crystal of C2UP2 was heated using an Oxford Cryosystems 700 heating device. The X-ray intensity data were measured on a Bruker SMART diffractometer (SMART-1K-CCD), at 533 K. The same data collection, reduction, and correction procedures as previously described were applied. The structure of the high temperature form was solved in the centrosymmetric $C2/m$ space group.

For the five studied structures no higher symmetry was found by checking the refined solutions with the ADDSYM algorithm in the program PLATON.¹⁹⁻²¹ Details of the data collection and refinement are given in Table 1. The heaviest atoms (U, P) were localized by means of direct methods using the SIR97 program.²² The oxygen, carbon, and nitrogen atoms were localized from difference Fourier maps. The positions of the hydrogen atoms were also determined from difference Fourier maps for C2UP2 and C2HP, but they were not found for the $CnUSP4$ compounds. Hydrogen atoms bonded to C atoms were allowed to ride during subsequent refinement, with $C-H = 0.99$ Å and $U_{iso}(H) = 1.2U_{eq}(C)$. All H atoms bound to N atoms were allowed to ride, with $N-H = 0.93$ Å and $U_{iso}(H) = 1.2U_{eq}(N)$. The H atom of the OH group was allowed to ride, with $O-H = 0.82$ Å and $U_{iso}(H) = 1.5U_{eq}(O)$.

The last cycles of refinement included atomic positions and anisotropic atomic displacement parameters for all atoms (except H) in C2UP2 and C2HP. Attempts to refine the oxygen atoms with anisotropic displacement parameters in the $CnUSP4$ compounds led to some non-definite oxygen atoms ($U < 0$) and did not improve the R factors, so anisotropic ADP for heavy atoms (U and P) and isotropic ADP for oxygen, carbon, and nitrogen atoms were included for refinement. Full-matrix least-squares structure refinements against F were carried out using the JANA2000 program.²³

Table 1. Details of the Data Collection and Refinement

	C4U5P4	C5U5P4	C2UP2 20 °C	C2UP2 260 °C	C2HP
Crystallographic Data					
chemical formula	C ₄ H ₁₆ N ₂ O ₂₇ P ₄ U ₅	C ₃ H ₁₆ N ₂ O ₂₇ P ₄ U ₅	C ₂ H ₁₀ N ₂ O ₈ P ₂ U	C ₂ H ₁₀ N ₂ O ₈ P ₂ U	C ₂ H ₁₁ N ₂ O ₄ P
formula weight (g.mol ⁻¹)	1838.2	1852.2	490.1	490.1	158.1
crystal system	orthorhombic	orthorhombic	triclinic	monoclinic	monoclinic
space group	<i>Cmc</i> ₂₁	<i>Cmc</i> ₂₁	<i>P</i> $\bar{1}$	<i>C2/m</i>	<i>P2</i> ₁ / <i>c</i>
Unit-Cell Dimensions					
<i>a</i> (Å)	15.5120(6)	15.520(2)	5.5737(1)	9.796(3)	10.615(2)
<i>b</i> (Å)	13.7953(5)	13.890(2)	5.6420(1)	5.562(2)	7.845(2)
<i>c</i> (Å)	13.0199(4)	13.077(2)	9.6856(1)	10.198(5)	8.334(2)
α (deg)			76.850(1)		
β (deg)			75.484(1)	112.219(5)	109.757(7)
γ (deg)			60.940(1)		
cell volume (Å ³)	2786.2(2)	2819.1(7)	255.72(1)	514.4(4)	653.2(3)
Z	4	4	1	2	4
density, calculated (g.cm ⁻³)	4.381	4.363	3.181	3.163	1.607
<i>F</i> (000)	3095	3119	222	424	336
Intensity Collection					
wavelength (Å)	0.71069 (Mo K α) for all				
θ range (deg)	2.0–27.4	2.0–25.9	2.2–32.3	8.6–29.7	2.0–37.8
data collected	–20 ≤ <i>h</i> ≤ 20 –17 ≤ <i>k</i> ≤ 16 –16 ≤ <i>l</i> ≤ 16	–19 ≤ <i>h</i> ≤ 19 –17 ≤ <i>k</i> ≤ 17 –16 ≤ <i>l</i> ≤ 16	–8 ≤ <i>h</i> ≤ 8 –8 ≤ <i>k</i> ≤ 8 –14 ≤ <i>l</i> ≤ 14	–13 ≤ <i>h</i> ≤ 13 –7 ≤ <i>k</i> ≤ 7 –13 ≤ <i>l</i> ≤ 14	–17 ≤ <i>h</i> ≤ 17 –13 ≤ <i>k</i> ≤ 13 –13 ≤ <i>l</i> ≤ 12
no. of reflections measured	11287	37024	19548	1845	15171
no. of independent reflections	3243	2838	1820	762	3223
redundancy					2.908
no. of unique reflections (<i>I</i> > 3 σ (<i>I</i>))	2699	2556	1820	751	2703
μ (MoK α) (mm ⁻¹)	29.30	28.96	16.21	16.12	0.37
<i>R</i> (<i>F</i> ²) _{int}	0.065	0.096	0.048	0.068	0.034
<i>R</i> (sig)	0.068	0.041	0.021	0.058	0.022
refinement					
twin fraction (%)	62	50			
no. of parameters	113	118	69	39	85
weighting scheme			1/ σ^2 for all		
<i>R</i> (<i>F</i>) obs/all	0.0368/0.0485	0.0267/0.0322	0.0142/0.142	0.046/0.047	0.0353/0.0430
w <i>R</i> (<i>F</i>) obs/all	0.0355/0.0374	0.0258/0.0263	0.0141/0.0141	0.047/0.047	0.0530/0.0535
max, min $\Delta\rho$ (e Å ⁻³)	1.96/–1.17	1.34/–1.19	0.64/–1.42	3.57/–2.67	0.81/–0.36

High Temperature X-ray Powder Diffraction. The high-temperature X-ray powder diffraction pattern was recorded using a BRUKER AXS D8 advance powder diffractometer (Cu K α radiation) in θ/θ Bragg–Brentano geometry equipped with an HTK 1200 Anton Paar chamber and a PSD detector (Super Speed VANTEC-1). The sample was deposited on an alumina holder. Experiments were performed over a temperature range from room temperature to 825 °C in an air atmosphere. The high-temperature X-ray diagrams (HTXRD) were recorded between 8 and 70° (2θ domain) with a step of 0.015° (2θ) and a counting time of 30 min per diagram.

Thermal Analyses. Thermogravimetric (TGA) and differential thermal (DTA) analyses experiments were performed on a Setaram coupled TGA-DTA 2–16.18 apparatus. Analyses were undertaken in air, with a heating rate of 5° min⁻¹, in platinum crucibles.

Spectroscopic Analyses. The purity of C2UP2 samples was checked using spectroscopic analyses. Diffuse Reflectance UV–visible Absorption was used to investigate the oxidation states of uranium and

Raman Scattering Spectroscopy was used to detect the various phosphate entities.

The UV–visible absorption spectra were recorded between 200 and 1800 nm using a Cary 6000i spectrometer. The instrument was equipped with an external integrating sphere (DRA-1800) to study the C2UP2 samples through diffuse reflectance. The spectra were plotted as the Kubelka–Munk function.

A Bruker RFS 100/S instrument was used as a near-IR FT-Raman spectrometer with a CW Nd:YAG laser at 1064 nm as the excitation source. A laser power of 100–200 mW was used. The spectra (3100–200 cm⁻¹) were recorded with a resolution of 2 cm⁻¹ using 600 scans.

RESULTS AND DISCUSSION

1. Diamine Stability and Decomposition during Synthesis.

Using linear alkyl diamines as templating agents in acidic medium leads to the formation of diprotonated diamine-uranyl-phosphates

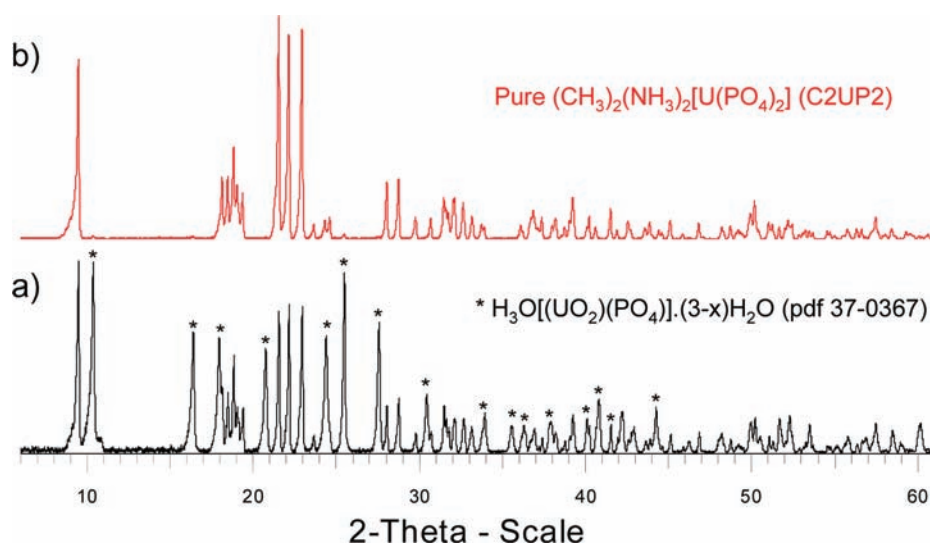


Figure 1. XRD pattern (a) of the solid composed of hydrogen uranyl phosphate tetrahydrate (PDF no. 37-0367) and C2UP2 obtained during the hydrothermal synthesis using ethylenediamine in a basic medium and (b) of the crushed single crystals of C2UP2 obtained after efficient separation of the phases by means of ultrasound decantation.

$(\text{CH}_2)_n(\text{NH}_3)_2\{\text{UO}_2(\text{H}_2\text{O})[(\text{UO}_2)(\text{PO}_4)]_4\} \cdot m\text{H}_2\text{O}$ for $n = 3-5$. In the same conditions, the linear diamines with $n = 6$ and 7 are not stable and give ammonium ions leading to the precipitation of ammonium uranyl phosphate trihydrate, $(\text{NH}_4)[(\text{UO}_2)(\text{PO}_4)] \cdot 3\text{H}_2\text{O}$.¹⁴ In neutral and basic media, all the linear diamines used except ethylenediamine undergo in situ decomposition into ammonium ions leading to the ammonium uranyl phosphate trihydrate powder formation. Amines decomposition under hydrothermal conditions has previously been observed.²⁴⁻²⁸ It is noteworthy that in our neutral and basic experimental conditions, ethylenediamine remains stable. Additionally, as the reduction of uranium from U(VI) to U(IV) occurs in the basic medium, that allows the formation of pink crystals of diprotonated ethylenediamine uranium(IV) phosphate crystals, $(\text{CH}_2)_2(\text{NH}_3)_2[\text{U}(\text{PO}_4)_2]$ (C2UP2). Such reduction of U(VI) to U(IV) under hydrothermal conditions has been previously reported in presence of homopiperazine or ethylenediamine in HF leading to $(\text{CH}_2)_2(\text{NH}_3)_2[\text{U}_2\text{F}_{10}]$.²⁹ Some other hydrothermal reactions conducted in presence of linear aliphatic diamines $(\text{CH}_2)_n(\text{NH}_2)_2$ ($n = 3, 4, 6$) or tris(2-aminoethyl)amine added with phosphoric acid³⁰ have also led to organic-inorganic U(IV) hybrid materials, but no reduction of uranium was reported since UO_2 and U_3O_8 were used as reactants.

The pink crystals were systematically accompanied with a yellow powder. Water was added to the solid mixture before being submitted to ultrasound decantation. The single crystals remain in suspension in the water when the yellow powder decants in the bottom of the tube leading to the separation of the two phases. That allows the identification of the yellow powder as hydrogen uranyl phosphate tetrahydrate¹⁵ (PDF no. 37-0367) and further characterization of the pure U(IV) compound (Figure.1). The stability of the ethylenediamine under hydrothermal conditions in basic medium was confirmed by the crystallization of ethylenediammonium hydrogen phosphate, $(\text{CH}_2)_2(\text{NH}_3)_2(\text{PO}_3\text{OH})$ (C2HP), resulting from the remaining solution.

2. Crystal Structure of the $\text{C}_n\text{U5P}_4$ ($n = 3, 4, 5$) Compounds. The three compounds contain uranium(VI) atoms present as uranyl UO_2^{2+} ions. They are built from uranophane-type

layers ${}^{\infty}[(\text{UO}_2)(\text{PO}_4)]^-$ formed by UO_7 pentagonal bipyramids and PO_4 tetrahedra. The orientation of the successive tetrahedra corresponds to the (uudd)(uddu) geometrical isomer¹³ which allows the formation of $[\text{UO}_6(\text{H}_2\text{O})]$ pillars between the layers and the creation of $\{[(\text{UO}_2)(\text{H}_2\text{O})][(\text{UO}_2)(\text{PO}_4)]_4\}^{2-}$ anionic frameworks (Figure 2). For $n = 4$ and 5, the diprotonated amines occupy the tunnels of these frameworks. For C5USP4, the diammonium pentane group half occupies two equivalent positions related by a m mirror parallel to the (1 0 0) plane containing the N1, C2, C3, and C5 atoms. No supplementary water molecule was localized within the channels leading to the general formula $(\text{CH}_2)_n(\text{NH}_3)_2\{\text{UO}_2(\text{H}_2\text{O})[(\text{UO}_2)(\text{PO}_4)]_4\}$. The $\text{C}_n\text{U5P}_4$ compounds are isotopic to the corresponding vanadates $\text{C}_n\text{U5V}_4$ [12]. The b and c unit cell parameters (Table 2) belong to the uranophane-type layer ${}^{\infty}[(\text{UO}_2)(\text{XO}_4)]^-$. They can be seen as the length of the ${}^1_{\infty}[\text{UO}_5]$ chain and of the direction perpendicular to it, within a unit cell, respectively. These parameters are not dependent on the alkyl chain length. They are systematically lower for $\text{X} = \text{P}$, which is in agreement with the reduction of the ionic radius and the XO_4 tetrahedron dimension from $\text{X} = \text{V}$ to $\text{X} = \text{P}$.

3. Crystal Structure of C2UP2. The crystal structure of $(\text{CH}_2)_2(\text{NH}_3)_2[\text{U}(\text{PO}_4)_2]$, C2UP2, at ambient temperature consists of a stack of anionic inorganic sheets, ${}^{\infty}[\text{U}(\text{PO}_4)_2]^{2-}$, and organic sheets of diprotonated ethylene diamine cations, $(\text{CH}_2)_2(\text{NH}_3)_2^{2+}$. The inorganic layer is built from UO_6 distorted octahedra linked by PO_4 tetrahedra. The asymmetric unit contains only one U atom on an inversion center and one P atom in a general position. The U atom is octahedrally coordinated to six oxygen atoms at distances of 2.210(3) ($2\times$), 2.225(1) ($2\times$) and 2.279(1) ($2\times$) Å. The average distance, 2.238(2) Å, is in agreement with the sum of ionic radii of six-coordinated U(IV) ($r = 0.89$ Å) and two-coordinated O ($r = 1.35$ Å)³¹ and is close to the value calculated in other uranium(IV) containing oxides, such as, for example, BaUO_3 with a perovskite-type structure, 2.204(7) Å.³² The valence bond sum of 4.28 $v.u.$, calculated using the data of Brese and O'Keefe,³³ confirms the (+IV) oxidation degree of U. The P atom is tetrahedrally coordinated by four oxygen atoms at nearly the same distance ($1.521(2)$ Å \leq P–O \leq $1.543(2)$ Å).

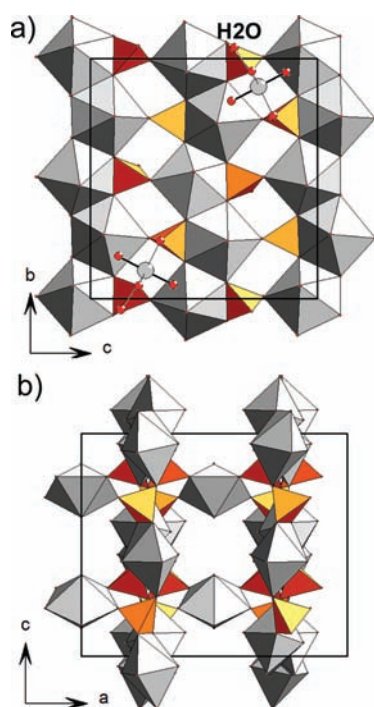


Figure 2. $\{[(\text{UO}_2)(\text{H}_2\text{O})][(\text{UO}_2)(\text{PO}_4)_4]^{2-}\}$ framework in the compounds C_nUSP_4 ($n = 3, 4, 5$) view along (a) the $[1\ 0\ 0]$ direction showing the uranophane-type uranyl phosphate layer and the $[\text{UO}_6(\text{H}_2\text{O})]$ pillars with uranyl bonds in thick lines, (b) the $[0\ 1\ 0]$ direction showing the connection between the layers by the $[\text{UO}_6(\text{H}_2\text{O})]$ pillars.

Table 2. Comparison of the Orthorhombic Unit Cell Parameters of C_nUSP_4 and C_nUSV_4 Compounds ($n = 3, 4, 5$)

	$a, \text{\AA}$	$b, \text{\AA}$	$c, \text{\AA}$	$V, \text{\AA}^3$
C3US V4	15.2754(2)	14.1374(2)	13.6609(2)	2950.13(7)
C3USP_4	15.3434(5)	13.8875(4)	13.0103(4)	2772.2 (2)
C4US V4	15.558(1)	14.1876(9)	13.6903(9)	3022.0(3)
C4USP_4	15.5120(6)	13.7953(5)	13.0199(4)	2786.2(2)
C5US V4	15.7246(7)	14.1208(5)	13.5697(5)	3013.1(2)
C5USP_4	15.520(2)	13.890(2)	13.077(2)	2819.1(7)

Three of them are shared with UO_6 octahedra leading to bond valence sums close to 2 *v.u.* (1.82, 1.96, and 2.01 *v.u.* for O2, O3, and O4, respectively). A UO_6 octahedron is connected to six other octahedra through six PO_4 tetrahedra to build a pseudo-hexagonal layer ${}_{\infty}[\text{U}(\text{PO}_4)_2]^{2-}$ (Figure 3a). This layer is similar to the one found in many layered phosphates and arsenates of tetravalent metals $M(\text{PO}_3\text{OH})_2 \cdot n\text{H}_2\text{O}$ ($M = \text{Si}, \text{Ge}, \text{Sn}, \text{Pb}, \text{Ti}, \text{Hf}$) isostructural with α -zirconium phosphate monohydrate $\text{Zr}(\text{PO}_3\text{OH})_2 \cdot \text{H}_2\text{O}$ (α -*ZrP*).^{34,35} However, in these compounds the oxygen not bonded to $M(\text{IV})$ belongs to a $\text{P}-\text{OH}$ group and gives a significantly longer $\text{P}-\text{O}$ bond than the others. On the contrary, in C2UP_2 the $\text{P}-\text{O}$ bond for the oxygen not bonded to $\text{U}(\text{IV})$ is slightly shorter than the others. That confirms the absence of the $\text{P}-\text{OH}$ group and an anionic layer of formula, ${}_{\infty}[\text{U}(\text{PO}_4)_2]^{2-}$, never reported up to now. Layers with $\text{P}-\text{OH}$ replaced by $\text{P}-\text{R}$ or $\text{P}-\text{OR}$ ($\text{R} =$ organic radical) have been reported in compounds $\text{Zr}(\text{PO}_3-\text{R})$ and $\text{Zr}(\text{PO}_3-\text{OR})$.^{36,37} The structure of $\text{U}(\text{PO}_3-\text{R})$ in which R is the phenyl radical $-\text{C}_6\text{H}_5$

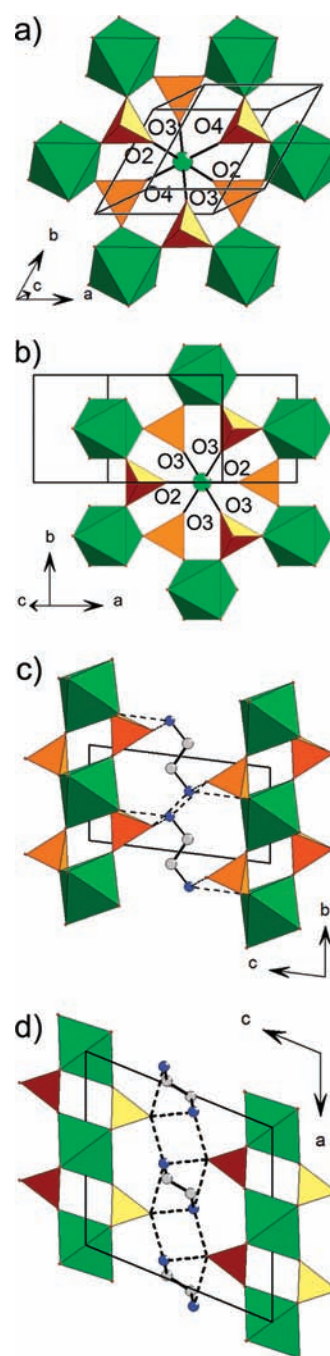


Figure 3. View of the uranium phosphate layer in the $(0\ 0\ 1)$ plane for $(\text{CH}_2)_2(\text{NH}_3)_2[\text{U}(\text{PO}_4)_2]$, C2UP_2 , at ambient temperature (a) and above $220\ ^\circ\text{C}$ (b). Projection along $[1\ 0\ 0]$ for the ambient temperature form (c) and along $[0\ 1\ 0]$ for the high temperature form (d) showing the stacking of the layers by means of the interlayer ethylene diammonium ions and the hydrogen bonds network.

has been determined from powder X-ray data.³⁸ This structure is similar to that of $\text{Zr}(\text{PO}_3-\text{C}_6\text{H}_5)$.³⁹ The existence of uranium hydrogenphosphates $\text{U}(\text{PO}_3\text{OH})_2 \cdot n\text{H}_2\text{O}$ has also been reported but not structurally characterized (see the reviews on $M(\text{IV})$ phosphates⁴⁰ and especially on $M(\text{IV})$ phosphates⁴¹). Therefore C2UP_2 represents the first example of organically templated $M(\text{IV})$ phosphate with α -*ZrP* type layered structure.

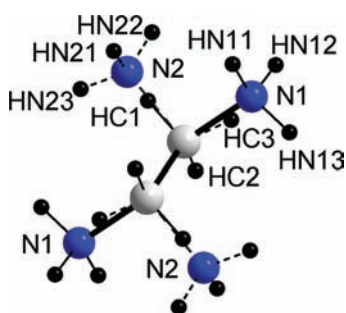


Figure 4. Disorder of the ethylene diammonium ions in C2UP2 at ambient temperature.

Table 3. Hydrogen Bond Characteristics in $(\text{CH}_2)_2(\text{NH}_3)_2[\text{U}(\text{PO}_4)_2]$, C2UP2

	N...O (Å)	H...O (Å)	N-H...O (deg)	s_{ij} ($\nu.u.$)
N2-HN23...O1	2.768 (5)	1.858(2)	165.2(3)	0.17
N2-HN22...O1	2.618(5)	1.754(2)	153.3(2)	0.23
N2-HN21...O2	2.989(6)	2.101(2)	159.3(3)	0.11
N1-HN13...O1	2.700(4)	1.827(2)	155.3(3)	0.18
N1-HN11...O1	2.595(6)	1.667(2)	174.4(3)	0.24
N1-HN12...O2	2.964(5)	2.078(2)	158.8(3)	0.11

The ethylenediammonium cations are located in the interlayer space. They are disordered on two positions $\text{C1}_2\text{N}_1\text{H}_{10}^{2+}$ and $\text{C1}_2\text{N}_2\text{H}_{10}^{2+}$ with a common C-C bond (Figure 4) and ensure the cohesion of the structure through N-H...O hydrogen bonds (Figure 3c and Table 3). The strongest hydrogen bonds involve the oxygen phosphate atom O1 which does not belong to the sheet. Including these hydrogen bonds to the valence bond calculation for O1 increases the bond valence sum from 1.25 to 1.66 $\nu.u.$ but O1 remains underbonded. That can be explained by the generally low valences of the N-H bonds calculated by means of Brown et al.'s method.⁴² The N-H are also a donor for a third weaker hydrogen bond with O2 as acceptor. That increases the bond valence sum of the atom O2 to 1.93 $\nu.u.$

The Raman spectrum confirms the presence of PO_4 groups in C2UP2. All the deformation and elongation modes of the P-O bond were assigned considering the data previously reported:⁴³⁻⁴⁶ (δ_s (380–472 cm^{-1}), δ_{as} (556–627 cm^{-1}), ν_s (950 and 960 cm^{-1}), and ν_{as} (1016–1072 cm^{-1})) (Figure 5a). The additional bands located at 1000, 1120, 1246–1339, and 1435–1475 cm^{-1} were attributed to the various vibrations (stretching, scissoring, wagging, and bending) of the C-C, C-N, NH_3^+ , and CH_2 bond belonging to the $(\text{CH}_2)_2(\text{NH}_3)_2^{2+}$ cations. No band characteristic of P_2O_7 entities or of uranyl cations (P-O-P at 703 and 739 cm^{-1} , and O=U=O at 850–870 cm^{-1}) was detected indicating that pure $(\text{CH}_2)_2(\text{NH}_3)_2[\text{U}(\text{PO}_4)_2]$ containing tetravalent uranium was obtained. The complementary UV-visible absorption spectra confirmed the reduction of U(VI) to U(IV) and the presence of U(IV) in C2UP2 (Figure 5b).

4. Thermal Study of C2UP2 and Phase Transition. Thermogravimetric analysis of C2UP2 (Figure 6) indicates a two steps decomposition with a total weight loss of 15.9% leading at above 850 °C to U(IV) diphosphate UP_2O_7 identified by the X-ray diffraction pattern of the final product (theoretical weight loss, 15.9%). The structure of UP_2O_7 was determined from powder X-ray data collected on a sample obtained by decomposition of

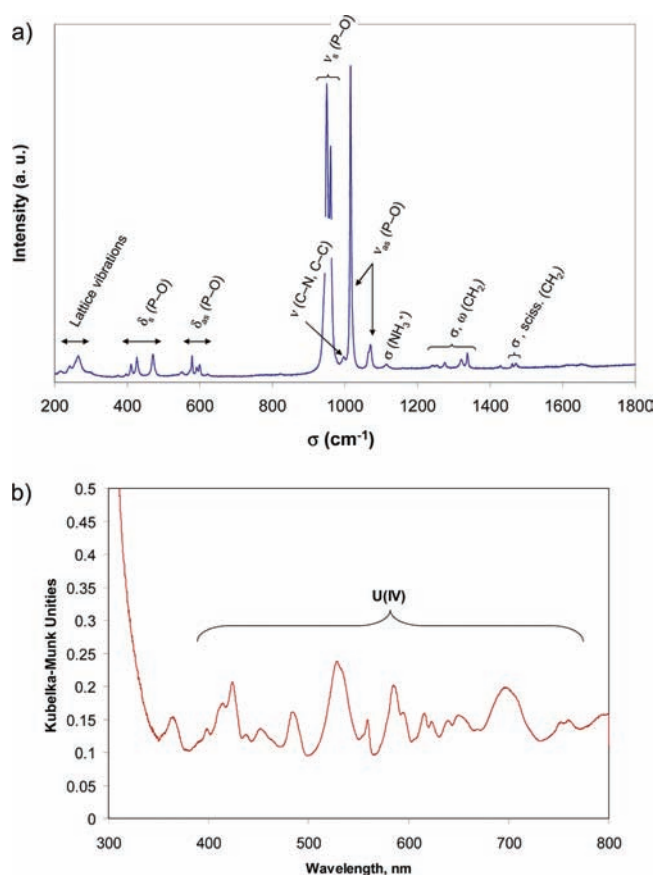


Figure 5. Raman spectrum (a) and diffuse reflectance UV-visible absorption spectrum of C2UP2 at room temperature.

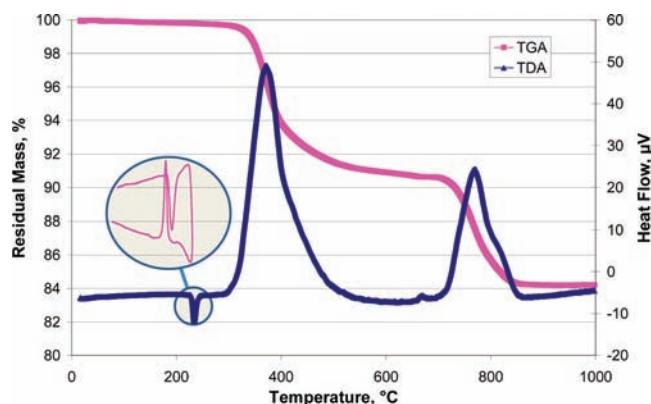


Figure 6. Thermal gravimetric (TGA) and differential (TDA) analyses of C2UP2 showing the two steps transformation into $\text{U}_2\text{P}_2\text{O}_7$. The inset shows the reversibility of the phase transition at about 230 °C.

$\text{U}(\text{O}_3\text{PC}_6\text{H}_5)$.³⁸ The decomposition of C2UP2 to UP_2O_7 was confirmed by the X-ray thermodiffraction (Figure 7) which indicates that the unidentified intermediate phase is amorphous.

DTA analysis shows a weak endothermic peak which appears at about 230 °C, before the two broad exothermic peaks at 400 and 770 °C corresponding to the two steps decomposition. This peak is not related to a weight loss but to a reversible phase transition confirmed by a change in the X-ray diffraction pattern on the HTXRD diagram.

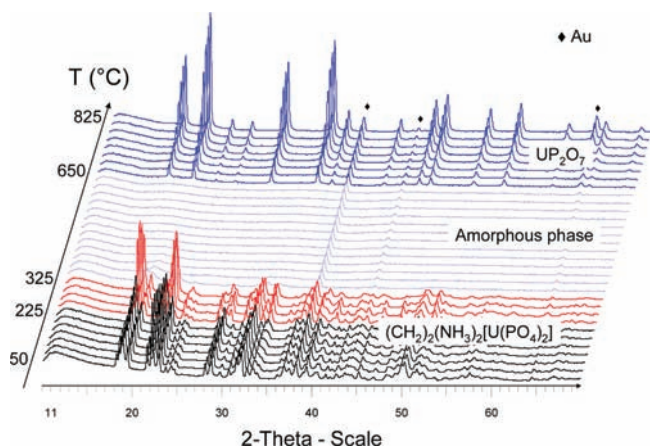


Figure 7. High-temperature X-ray powder diffraction pattern of C2UP2.

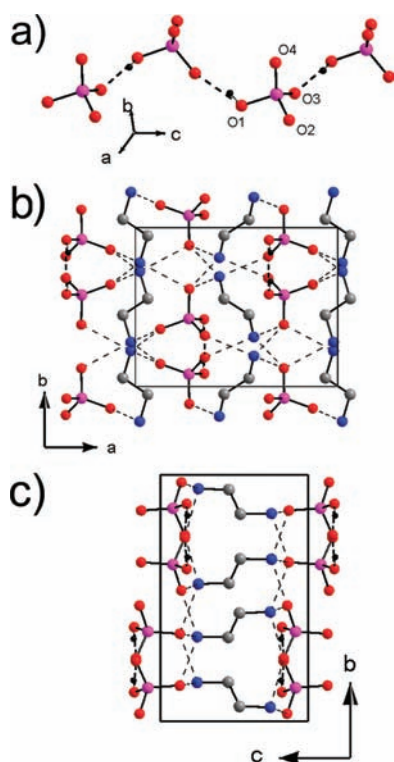


Figure 8. Connection of the PO_4H tetrahedra through strong $\text{O1}-\text{H}\cdots\text{O3}$ bonds to create ${}^1\infty[\text{PO}_4\text{H}]^{2-}$ infinite chains running down the $[0\ 0\ 1]$ direction (a) and view along the $[0\ 0\ 1]$ (b) and $[1\ 0\ 0]$ (c) directions showing the linkage of the hydrogenophosphates chains by the ethylenediammonium ions through $\text{N}-\text{H}\cdots\text{O}$ bonds (hydrogen atoms of the ethylenediammonium ions are omitted for clarity) in the two forms of ethylenediammonium monohydrogen phosphate ((a) and (b) this study, (c) ref 47).

The powder X-ray pattern recorded at 260 °C was fully indexed with a C-centered monoclinic cell. The unit cell parameters were refined to $a = 9.799(4)$, $b = 5.58(3)$, $c = 11.184(9)$ Å, $\beta = 122.21(5)^\circ$. These results were confirmed by the study of a single crystal heated at 260 °C. The structure was determined in the centrosymmetric space group $C2/m$ (Table 1). The main features of the structural arrangement are of course maintained

with a staking of α -ZrP type uranium(IV) layers (Figure 3b). The major differences concern the relative positions of the successive layers and the positions and orientations of the interlayer ethylene diammonium ions which lead to a different hydrogen bonds network (Figure 3d).

5. Crystal Structure of C2HP. The unit cell of C2PH contains four hydrogen phosphate ions and four ethylenediammonium ions located in two crystallographically independent positions leading to the formula $(\text{CH}_2)_2(\text{NH}_3)_2^{2+}(\text{PO}_3\text{OH})^{2-}$. In the tetrahedral geometry of the hydrogen phosphate ion, the interatomic angles are in agreement with the values of the literature. One P–O bond is longer (1.584(4) Å) than the others (in the range 1.511(1) to 1.521(1) Å), that is typical of a (PO_3OH) group. The two independent ethylenediammonium ions possess an inversion center and the same geometrical features with C–C, C–N distances and N–C–C angle of 1.501(2), 1.478(2) Å, $110.8(1)^\circ$ and 1.510(2), 1.476(2) Å, $110.3(1)^\circ$ for $((\text{C1H}_2)_2(\text{N1H}_3)_2)^{2+}$ and $((\text{C2H}_2)_2(\text{N2H}_3)_2)^{2+}$, respectively. The PO_3OH tetrahedra are linked together through strong $\text{O1}-\text{H}\cdots\text{O3}$ bonds ($\text{O1}-\text{O3} = 2.592(2)$ Å) to create an infinite chain running down the $[0\ 0\ 1]$ direction (Figure 8a). Sheets of infinite ${}^1\infty[\text{PO}_3\text{OH}]^{2-}$ chains parallel to the (001) plane at $x = 0.25$ and 0.75 are stacked with sheets containing $(\text{C1H}_2)_2(\text{N1H}_3)_2^{2+}$ and $(\text{C2H}_2)_2(\text{N2H}_3)_2^{2+}$ at $x = 0.5$ and $x = 0$, respectively. The connection between successive sheets is ensured by hydrogen $\text{N}-\text{H}\cdots\text{O}$ bonds, each ammonium ion being involved in three hydrogen bonds (Figure 8b). This structure is isotopic to the corresponding arsenate compound⁴⁷ but different from the previously reported ethylenediammonium monohydrogen phosphate^{47,48} also built from infinite ${}^1\infty[\text{PO}_4\text{H}]^{2-}$ chains but with another orientation of non-centrosymmetric $((\text{C1H}_2)_2(\text{C2H}_2)_2(\text{N1H}_3)_2(\text{N2H}_3)_2)^{2+}$ ions (Figure 8c).

CONCLUSION

Hydrothermal syntheses using linear alkyl diamines $\text{C}_n\text{H}_{2n+4}\text{N}_2$ as templating agents in acidic medium lead, for $n = 3-5$, to the formation of diprotonated diamine-uranyl-phosphates $(\text{C}_n\text{H}_{2n+6}\text{N}_2)\cdot\{\text{UO}_2(\text{H}_2\text{O})[(\text{UO}_2)(\text{PO}_4)]_4\} \cdot m\text{H}_2\text{O}$ isostructural with the vanadate analogues with structures based on $\{[(\text{UO}_2)(\text{H}_2\text{O})]-(\text{UO}_2)(\text{PO}_4)]_4\}^{2-}$ frameworks. For the same diamines in basic or neutral medium, in situ decomposition of the amines into ammonium ions leads to the precipitation of ammonium uranyl phosphate trihydrate. In basic conditions, ethylenediamine ($n = 2$) remains stable leading to the formation of ethylenediammonium uranium(IV) phosphate, $(\text{CH}_2)_2(\text{NH}_3)_2[\text{U}(\text{PO}_4)_2]$ and to the formation of $(\text{CH}_2)_2(\text{NH}_3)_2(\text{PO}_3\text{OH})$ which crystallizes from the mother liquor decanted from the $(\text{CH}_2)_2(\text{NH}_3)_2[\text{U}(\text{PO}_4)_2]$ crystals. The structure of the latter is built on anionic uranium(IV) layers of α -ZrP type interleaved by ethylene diammonium ions. $(\text{CH}_2)_2(\text{NH}_3)_2[\text{U}(\text{PO}_4)_2]$ is the first example of the direct synthesis of a uranium(IV) phosphate with an anionic α -ZrP type layer by using a templating agent. The unexpected in situ reduction of U(VI) to U(IV) in the presence of ethylenediamine under the mild hydrothermal conditions reported herein opens a new route for the synthesis of original compounds.

At 220 °C, $(\text{CH}_2)_2(\text{NH}_3)_2[\text{U}(\text{PO}_4)_2]$ undergoes a reversible phase transition from $P\bar{1}$ to $C2/m$ symmetry and decomposes into UP_2O_7 at 850 °C. The decomposition occurs in a two steps process leading to an intermediate amorphous compound which remains under study.

■ ASSOCIATED CONTENT

S Supporting Information. Crystallographic data in CIF format. This material is available free of charge via the Internet at <http://pubs.acs.org>.

■ AUTHOR INFORMATION

Corresponding Author

*Phone: +33 3 20 33 64 35 Fax: +33 3 20 43 68 14 e-mail: murielle.rivenet@ensc-lille.fr.

■ ACKNOWLEDGMENT

The authors thank Myriam Moreau (CCM LASIR, USTL) and Alain Moissette (LASIR, USTL) for their help in the spectroscopic measurements. This work benefited from the financial support of Agence Nationale de la Recherche (ANR-08-BLAN-0216).

■ REFERENCES

- (1) Burns, P. C.; Miller, M. L.; Ewing, R. C. *Can. Mineral.* **1996**, *34*, 845. Burns, P. C.; Ewing, R. C.; Hawthorne, F. C. *Can. Mineral.* **1997**, *35*, 1551. Burns, P. C. *Can. Mineral.* **2005**, *43*, 1839.
- (2) Locock, A. J.; Burns, P. C. *J. Solid State Chem.* **2004**, *177*, 2675.
- (3) Rivenet, M.; Vigier, N.; Roussel, P.; Abraham, F. *J. Solid State Chem.* **2007**, *180*, 713.
- (4) Saadi, M.; Dion, C.; Abraham, F. *J. Solid State Chem.* **2000**, *150*, 72.
- (5) Locock, A. J.; Burns, P. C. *J. Solid State Chem.* **2002**, *163*, 275.
- (6) Locock, A. J.; Burns, P. C. *J. Solid State Chem.* **2003**, *176*, 18.
- (7) Locock, A. J.; Burns, P. C. *J. Solid State Chem.* **2002**, *167*, 226.
- (8) Locock, A. J.; Burns, P. C. *J. Solid State Chem.* **2003**, *175*, 372.
- (9) Locock, A. J.; Burns, P. C. *Z. Kristallogr.* **2004**, *219*, 259.
- (10) Danis, J. A.; Runde, W. H.; Scott, B.; Fettingner, J.; Eichhorn, B. *Chem. Commun.* **2001**, *22*, 2378.
- (11) Jouffret, L.; Shao, Z.; Rivenet, M.; Abraham, F. *J. Solid State Chem.* **2010**, *183*, 2290.
- (12) Jouffret, L.; Rivenet, M.; Abraham, F. *J. Solid State Chem.* **2010**, *183*, 84.
- (13) Jouffret, L.; Rivenet, M.; Abraham, F. *IOP Conf. Series: Mater. Sci. Eng.* **2010**, *9*, 012028.
- (14) Botto, I. L.; Baran, E. J.; Aymonino, P. J. *Z. Chem.* **1975**, *16*, 163. Fitch, A. N.; Fender, B. E. F. *Acta Crystallogr.* **1983**, *C39*, 162.
- (15) Atencio, D. *Mineral. Rec.* **1988**, *19*, 249. Morosini, B. *Acta Crystallogr.* **1978**, *B34*, 3732–3734. Pham-Thi, M.; Colomban, P. *J. Less—Common Met.* **1985**, *108*, 189.
- (16) COSMO Bruker program, V1.56; Bruker AXS, Inc: Madison, WI, 1999–2006
- (17) SAINT Plus, Version 6.22; Bruker Analytical X-ray Systems: Madison, WI, 2001.
- (18) SADABS, Version 2.03; Bruker Analytical X-ray Systems: Madison, WI, 2001.
- (19) LePage, Y. *J. Appl. Crystallogr.* **1987**, *20*, 264.
- (20) Spek, A. L. *J. Appl. Crystallogr.* **1988**, *21*, 578.
- (21) Spek, A. L. *PLATON*; Utrecht University: Utrecht, The Netherlands, 2001.
- (22) Altomare, A.; Burla, M. C.; Camalli, M.; Cascarano, G. L.; Giacovazzo, C.; Guagliardi, A.; Moliterni, A. G.; Polidori, G.; Spagna, R. *J. Appl. Crystallogr.* **1999**, *32*, 115.
- (23) Petricek, V.; Dusek, M.; Palatinus, L. *JANA2000*; Institute of Physics: Praha, Czech Republic, 2005.
- (24) Chippindale, A. M.; Walton, R. L. *J. Chem. Soc., Chem. Commun.* **1994**, 2453.
- (25) Chippindale, A. M.; Cowley, A. R.; Walton, R. L. *J. Mater. Chem.* **1996**, *6*, 611.
- (26) Trombe, J. C.; Thomas, P.; Brouca-Cabarrecq, C. *Solid State Sci.* **2001**, *3*, 309.
- (27) Bircsak, Z.; Harrison, W. T. A. *Acta Crystallogr.* **1998**, *C54*, 1383.
- (28) Fourcade-Cavillou, F.; Trombe, J. C. *Solid State Sci.* **2002**, *4*, 1199.
- (29) Almond, P. M.; Deakin, L.; Porter, M. J.; Mar, A.; Albrecht-Schmitt, T. E. *Chem. Mater.* **2000**, *12*, 3208.
- (30) Francis, R. J.; Halasyamani, P. S.; O'Hare, D. *Chem. Mater.* **1998**, *10*, 3131.
- (31) Shannon, R. D. *Acta Crystallogr.* **1976**, *A32*, 751.
- (32) Barrett, S. A.; Jacobson, A. J.; Tofield, B. C.; Fender, B. E. F. *Acta Crystallogr.* **1982**, *B38*, 2775.
- (33) Brese, N. E.; O'Keefe, M. *Acta Crystallogr.* **1991**, *B47*, 192.
- (34) Clearfield, A.; Smith, G. D. *Inorg. Chem.* **1969**, *8*, 431.
- (35) Troup, J. M.; Clearfield, A. *Inorg. Chem.* **1977**, *16*, 3311.
- (36) Yamanaka, S. *Inorg. Chem.* **1976**, *15*, 2811. Alberti, G.; Constantino, U.; Allulli, S.; Tomassini, N. *J. Inorg. Nucl. Chem.* **1978**, *40*, 1113. Yamanaka, S. *Inorg. Chem.* **1976**, *15*, 2811. Dines, M. B.; Cooksey, R. E.; Griffith, P. C.; Lane, R. H. *Inorg. Chem.* **1983**, *22*, 1003. Ortiz-Avila, C. Y.; Clearfield, A. *J. Chem. Soc., Dalton Trans.* **1989**, 1617.
- (37) Casciola, M.; Capitani, D.; Donnadio, A.; Munari, G.; Pica, M. *Inorg. Chem.* **2010**, *49*, 3329.
- (38) Cabeza, A.; Aranda, M. A. G.; Cantero, F. M.; Lozano, D.; Martinez-Lara, M.; Bruque, S. *J. Solid State Chem.* **1996**, *121*, 181.
- (39) Poojary, M. D.; Hu, H.-L.; Campbell, F. L., III; Clearfield, A. *Acta Crystallogr.* **1993**, *B49*, 996.
- (40) Brandel, V.; Dacheux, N. *J. Solid State Chem.* **2004**, *177*, 4743; **2004**, *177*, 4755.
- (41) Brandel, V.; Dacheux, N. *J. Solid State Chem.* **1996**, *121*, 467.
- (42) Brown, I. D.; Altermatt, D. *Acta Crystallogr.* **1985**, *B41*, 244.
- (43) Clavier, N.; du Fou de Kerdaniel, E.; Dacheux, N.; Le Coustumer, P.; Drot, R.; Ravau, J.; Simoni, E. *J. Nucl. Mater.* **2006**, *349*, 304.
- (44) Dacheux, N.; Grandjean, S.; Rousselle, J.; Clavier, N. *Inorg. Chem.* **2007**, *46*, 10390.
- (45) Terra, O.; Dacheux, N.; Clavier, N.; Podor, R.; Audubert, F. *J. Am. Ceram. Soc.* **2008**, *91* (11), 3673.
- (46) Ingham, B.; Chong, S. V.; Tallon, J. L. *J. Phys. Chem.* **2005**, *B109*, 4936.
- (47) Averbuch-Pouchot, M. T.; Durif, A. *Acta Crystallogr.* **1987**, *C43*, 1894.
- (48) Choudhury, A.; Natarajan, S.; Rao, C. N. R. *Int. J. Inorg. Mater.* **2000**, *2*, 87.